Spin−Orbit Effects on Hyperfine Coupling Tensors in Transition Metal Complexes Using Hybrid Density Functionals and Accurate Spin−Orbit Operators

Christian Remenyi,[†] **Roman Reviakine,**[†] **Alexei V. Arbuznikov,**[†] **Juha Vaara,**[‡] **and Martin Kaupp***[,†]

Institut für Anorganische Chemie, Universität Würzburg, Am Hubland, D-97074 Würzburg, Germany, and Laboratory of Physical Chemistry, Department of Chemistry, P.O. Box 55 (A. I. Virtasen aukio 1), FIN-00014 University of Helsinki, Finland

Received: February 10, 2004; In Final Form: March 31, 2004

A coupled-perturbed Kohn−Sham treatment for the calculation of hyperfine tensors has been implemented into the MAG-ReSpect program. It treats spin−orbit contributions to hyperfine tensors by a combination of accurate and efficient approximations to the one- and two-electron spin−orbit Hamiltonians: (a) by the all-electron atomic mean-field approximation, and (b) by spin−orbit pseudopotentials. In contrast to a previous implementation, the code allows the use of hybrid functionals and lifts restrictions in the orbital and auxiliary basis sets that may be employed. Validation calculations have been performed on various transition metal complexes, as well as on a series of small diatomic molecules. In the case of a series of copper(II) complexes, the spin−orbit contributions are large, and their inclusion is essential to achieve agreement with experiment. Calculations with spin−orbit pseudopotentials allow the efficient simultaneous introduction of scalar relativistic and spin−orbit effects in the case of light nuclei in the neighborhood of heavy atoms.

1. Introduction

Hyperfine coupling (HFC) tensors are sensitive probes of the spin-density distribution in molecules and thereby provide a large part of the information of an electron paramagnetic resonance (EPR) spectrum. In view of the importance of EPR spectroscopy in many areas of chemistry, biochemistry or materials science, accurate quantum-chemical calculations of hyperfine tensors are of central importance in the prediction and analysis of EPR spectra in various fields.[1] Such computations have turned out to be particularly difficult for transition metal complexes. As extended post-Hartree−Fock ab initio methods are computationally too demanding to be applied to transition metal systems of chemically relevant size, density functional theory (DFT) offers currently the only practical approach to reasonably accurate calculations of hyperfine tensors in transition metal systems. Particularly the isotropic hyperfine couplings, however, are frequently difficult to obtain accurately, due to the need to describe well the important core−shell spin polarization without introducing spin contamination due to exaggerated valence-shell spin polarization.[2,3] Currently, there is no perfect exchange-correlation functional available that would provide consistently good performance for hyperfine couplings in all cases.

The second problem to be dealt with are relativistic effects on the HFC tensors, including both scalar (spin-free) relativistic (SR) and spin−orbit (SO) effects. These are known to influence already the HFC results for 3d transition metal complexes appreciably, and they have to be considered for quantitative evaluation. In this article we concentrate on a new perturbation-theoretical implementation of SO effects on HFC tensors.

The theoretically most satisfying approach toward relativistic calculation of HFC tensors would be a fully relativistic treatment at the four-component level (as recently reported at the Dirac−Fock level).[4] However, this is currently too demanding to be of use for larger systems, in particular because the inclusion of electron correlation and spin polarization is required. An alternative is provided by transformed two-component Hamiltonians such as the zeroth-order regular approximation (ZORA)[5] or the Douglas−Kroll−Hess (DKH) method.[6] A ZORA implementation in the ADF program has become quite popular for HFC calculations by DFT.[7,8] An as yet unsolved problem is, however, that currently a two-component treatment is only available at the spin-restricted (ROKS) level (whereas one-component ZORA calculations may include spin polarization at the unrestricted Kohn−Sham (UKS) level). Provided the SO coupling is not too large, the perturbative inclusion of SO effects offers a practical way to include both SO contributions and spin polarization within a UKS-based treatment.

Several such second-order perturbation theory DFT approaches to calculate SO corrections to HFC tensors have been proposed. Though most implementations have relied on semiempirical one-electron SO operators,[2,9−11] we have recently reported[12] the first calculations using accurate ab initio approximations to the full microscopic one- and two-electron Breit−Pauli SO Hamiltonian. These were (a) the all-electron atomic mean-field approximation,[13] and (b) SO pseudopotentials ("effective core potentials", SO-ECPs).[14−17] Test calculations of HFC tensors in a series of model systems, using local density (LDA) and generalized gradient-approximation (GGA) exchange-correlation functionals, have provided reasonable agreement between these two approaches, as well as with experiment, provided that the underlying nonrelativistic (NR) parts of the HFC tensor were computed accurately.

Our implementation of ref 12 suffered still from limitations in the underlying deMon-KS[18] and deMon-NMR-EPR[19] codes. These were (a) the restriction of both orbital basis sets and auxiliary basis sets for the fit of electron density and exchange-correlation potential to angular momentum $l \leq 2$, and (b)

---

* Corresponding author. E-mail: kaupp@mail.uni-wuerzburg.de.
[†] Universität Würzburg.
[‡] University of Helsinki.

10.1021/jp049395p CCC: $27.50

restriction to LDA and GGA functionals, due to the lack of four-center two-electron integrals. This precludes the use of hybrid functionals that include a fraction of exact exchange. As the recent results of Neese[10] suggested larger SO corrections to HFC tensors in transition metal complexes when using hybrid functionals (and thereby potentially better agreement with experiment), we have now transferred our accurate ab initio type implementation of ref 12 to the framework of the MAG-ReSpect program,[20] which does not suffer from the above-mentioned restrictions. We report here the first validation study of the new implementation, mainly for transition metal complexes, comparing GGA and hybrid functionals.

2. Theory

The details of the second-order perturbation treatment of HFC tensors have been provided in refs 10 and 12. Here we repeat only the salient features of the approach.[12] The part of the ESR spin Hamiltonian[21] pertaining to hyperfine coupling is usually written as

$$H_{\mathrm{K}}^{\mathrm{hf}} = S\cdot\mathbf{A}_{\mathrm{K}}\cdot I_{\mathrm{K}} \tag{1}$$

Using the Breit−Pauli Hamiltonian and a vector potential corresponding to a pointlike magnetic dipole moment of nucleus K, one ends up with two contributions to lowest order (up to α^2), the isotropic Fermi-contact term A^{FC}, and the anisotropic dipolar coupling, $\mathbf{A}^{\mathrm{dip}}$. Within a single-determinantal LCAO approach, these may be expressed as

$$A_{\mathrm{K}}^{\mathrm{iso}} = A_{\mathrm{K}}^{\mathrm{FC}} = \frac{4\pi}{3}\alpha^2 g_{\mathrm{e}}\gamma_{\mathrm{K}}\frac{1}{2\langle S_Z\rangle}\sum_{\mu,\nu}P_{\mu\nu}^{\alpha-\beta}\langle\chi_\mu|\delta(\mathbf{r}_{\mathrm{K}})|\chi_\nu\rangle \tag{2}$$

$$A_{\mathrm{K},\mu,\nu}^{\mathrm{dip}} = \frac{1}{2}\alpha^2 g_{\mathrm{e}} g_{\mathrm{K}}\gamma_{\mathrm{K}}\frac{1}{2\langle S_Z\rangle}\sum_{\mu,\nu}P_{\mu,\nu}^{\alpha-\beta}\langle\chi_\mu|r_{\mathrm{K}}{}^{-5}(r_{\mathrm{K}}{}^2\delta_{\mu,\nu} - 3r_{\mathrm{K},\nu}r_{\mathrm{K},\nu})|\chi_\nu\rangle \tag{3}$$

where γ_{K} is the gyromagnetic ratio of nucleus K, and g_{e} is the free-electron g value (2.002319...). $\langle S_Z\rangle$ is the maximum value of the spin projection and $P_{\mu,\nu}^{\alpha-\beta}$ is the spin density matrix in the atomic orbital basis $\{\chi_\mu\}$. A^{FC} and $\mathbf{A}^{\mathrm{dip}}$ contribute to the nonrelativistic (NR) part of the HFC tensor.

The dominant SO correction term arises as a second-order coupling term. To enable calculations with hybrid functionals, a coupled-perturbed Kohn−Sham (CPKS) treatment had to be implemented into the MAG-ReSpect program. Our CPKS implementation for SO corrections to HFCs in MAG-ReSpect is based on our analogous **g** tensor code[22] and differs from Neese's previous implementation[10] (which has been the first CPKS treatment of SO corrections to HFC tensors) mainly by the approximations in the SO matrix elements (see below). In this scheme the SO contribution is written as a cross term between one- and two-electron SO Hamiltonian h^{SO} and the perturbed Fock operator F'_K:

$$A_{\mathrm{K,uv}}^{\mathrm{SO-I(1)}} + A_{\mathrm{K,uv}}^{\mathrm{SO-I(2)}} = \frac{1}{2}\alpha^4 g_{\mathrm{e}}\gamma_{\mathrm{K}}\frac{1}{2\langle S_Z\rangle}\times \left[\sum_k^{\mathrm{occ}(\alpha)}\sum_a^{\mathrm{virt}(\alpha)}\frac{\langle\psi_k^\alpha|h_{\mathrm{u}}^{\mathrm{SO}}|\psi_a^\alpha\rangle\langle\psi_a^\alpha|F'_{\mathrm{K,v}}|\psi_k^\alpha\rangle}{\epsilon_k^\alpha - \epsilon_a^\alpha} - \sum_k^{\mathrm{occ}(\beta)}\sum_a^{\mathrm{virt}(\beta)}\frac{\langle\psi_k^\beta|h_{\mathrm{u}}^{\mathrm{SO}}|\psi_a^\beta\rangle\langle\psi_a^\beta|F'_{\mathrm{K,v}}|\psi_k^\beta\rangle}{\epsilon_k^\beta - \epsilon_a^\beta}\right] \tag{4}$$

with $F'_{K,\mathrm{v}} = (l_{\mathrm{v}}/r^3) - a_0\sum_{k=1}^{n/2}K'_{k,\mathrm{v}}$, where (l_{v}/r^3) is the paramagnetic nuclear-spin electron-orbit (PSO) operator, $K'_{k,\mathrm{v}}$ is the response exchange operator (summed over all $n/2$ occupied orbitals), and a_0 is the weight of HF exchange depending on the specific hybrid functional used. In the case of "nonhybrid" functionals that do not depend on nonlocal Hartree−Fock exchange, such as the BP86 GGA functional, an uncoupled DFT approach is appropriate (possibly modified by Malkin's sum-over-states density functional perturbation theory correction terms[23]), as detailed in ref 12. Because a_0 in this case is zero, the second part of the expression for F'_k vanishes, leading to the common PSO operator. For a fuller description of the symbols appearing in eq 4, please refer to ref 12.

An additional diamagnetic part (with both one and two electron contributions) which gives an additional first-order contribution to **A**, is neglected due to its general smallness.[12] The total **A** tensor may thus be expressed as

$$\mathbf{A}_{\mathrm{K}} = \mathbf{A}_{\mathrm{K}}^{\mathrm{NR}} + \mathbf{A}_{\mathrm{K}}^{\mathrm{SO}} \tag{5}$$

For better comparison with experimental values the SO correction to **A** is given in terms of an isotropic pseudocontact (PC) and traceless dipolar ("dip,2") term.

$$\mathbf{A}_{\mathrm{K}}^{\mathrm{SO}} = \mathbf{A}_{\mathrm{K}}^{\mathrm{PC}} + \mathbf{A}_{\mathrm{K}}^{\mathrm{dip,2}} \tag{6}$$

For axially symmetric sites, $\mathbf{A}^{\mathrm{dip}}$ and $\mathbf{A}^{\mathrm{dip,2}}$ refer to the principal components of the corresponding traceless tensors ($-\mathbf{A}^{\mathrm{dip}}$, $-\mathbf{A}^{\mathrm{dip}}$, $2\mathbf{A}^{\mathrm{dip}}$) where $2\mathbf{A}^{\mathrm{dip}}$ is the component in the direction along the molecular axis. For axially nonsymmetric sites the three principal components of the traceless tensors are presented individually.

3. Computational Details

In contrast to the previous deMon implementation,[12] the current work did not rely on fitting of charge density or exchange-correlation potential but computed four-center two-electron integrals explicitly. The BP86 GGA functional[24−26] and the B3PW91 hybrid functional[27,28] were compared. Unless noted otherwise, in all DFT calculations an integration grid with 64 radial points with fine angular quadrature (corresponding to ca. 5000−5500 grid points per atom) has been used. In addition, in some cases the B3LYP functional[27,29] was used for comparison in calculations of the NR part of the HFC tensors. In the latter calculations (and in a few comparative BP86-based calculations), the SCF part was done with the Gaussian98 program[30] (the *tight* program option was used for SCF convergence criteria, corresponding to 10^{-8} au in energies and densities), and the Kohn−Sham orbitals were transferred to MAG-ReSpect by suitable interface routines[23] (the LYP correlation functional is currently being implemented in ReSpect).

For 3d transition metals, a (15s11p6d)/[9s7p4d] basis constructed specifically for HFC calculations[2] has been used. Ligand atoms were treated by Huzinaga−Kutzelnigg-type basis sets BII and BIII.[31,32] For a series of diatomics we compare all-electron and ECP calculations (the SCF part was done with the Gaussian98 program[30] in these cases). As in ref 12, all-electron calculations used the BIII type basis[31,32] for the lighter atoms, with basis sets by Fægri[33] for the heavier elements in an analogous BIII-type contraction (denoted as FIII). Scalar relativistic ECPs and corresponding SO-ECPs for Ga, In, Rh (small-core definition), as well as for Br and I (7-valence-electron treatment) were taken from refs 14−17.

TABLE 1: Metal Hyperfine Coupling Tensors (MHz) in Carbonyl Complexes[a]

			isotropic part				dipolar (anisotropic) part			
complex			A^{FC}	A^{PC}	total	exp	A^{dip}	$A^{dip,2}$	total	exp
$[Co(CO)_4]$	ref 2	BP86	−11	70[b]	58	−47.8, −52(1)[42]	152	−42[b]	110	110[42]
		B3PW91	−75	70[b]	5		146	−42[b]	102	
	this work	BP86	−12	31	19		151	−14	137	
		B3PW91	−73	48	−25		144	−18	126	
$[Ni(CO)_3H]$	ref 2	BP86	22	−27[b]	−4	9.0(2)[43]	−50	16[b]	−33	−44.0(2)[43]
		B3PW91	34	−27[b]	7		−57	16[b]	−40	
	this work	BP86	15	−8	7		−50	4	−46	
		B3PW91	23	−15	8		−56	6	−50	
$[Fe(CO)_5]^+$	ref 2	BP86	0	5[b]	5	−2.2[44]	18	−3[b]	15	15.4[44]
		B3PW91	−5	5[b]	0		19	−3[b]	16	
	this work	BP86	0	2	2		18	−1	17	
		B3PW91	−5	3	−2		19	−2	17	
$[Mn(CO)_5]$	ref 2	BP86	3	21[b]	24	−2.8, 0.6, 5.6[45]	96	−13[b]	83	90(8)−92(6)[45]
		B3PW91	−12	21[b]	9		96	−13[b]	83	
	this work	BP86	6	2	8		96	−2	94	
		B3PW91	−4	2	−2		95	−2	93	

[a] (15s11p6d)/[9s7p4d] basis set for the metal atoms, BIII basis sets for the main group elements. [b] Semiempirical estimates of SO corrections.

The effective one-electron/one-center mean-field SO operators were computed with the AMFI program.[34] In cases where ECPs and SO-ECPs were used on the heavy atoms, AMFI SO operators were employed on the light atoms. Details on and the excellent performance of the AMFI approximation have been discussed for various other magnetic resonance parameters, such as SO corrections to NMR chemical shifts[35] and electronic **g** tensors.[36]

In the case of metal carbonyl and manganese complexes, molecular structures used for the hyperfine structure calculations were taken from experiment where available. Where not, the DFT-optimized structures of ref 2 were used. Structures of Cu complexes have been optimized in unrestricted Kohn−Sham calculations with the BP86 functional using the Turbomole 5.6 program[37] and TZVP basis sets[38] for all atoms. The Coulomb term was approximated by the resolution of the identity (RI) method (density fitting with a TZVP auxiliary basis set).[39] We verified that the structures (Cartesian coordinates available as Supporting Information Table 6S) obtained are closely similar to those used by Neese.[10] Structures of the series of diatomics studied are those employed and discussed in ref 12.

All HFC tensor results are reported in megahertz.

4. Results and Discussion

4.1. Carbonyl Complexes: Comparison to Semiempirical SO Corrections. In Table 1, comparison is made for a number of carbonyl complexes to first-order NR results of ref 2, augmented by semiempirical SO corrections. Both the BP86 GGA functional and the hybrid B3PW91 functional have been used. As expected, the anisotropic part of the NR HFC tensor (due to the spin-dipolar interaction) of the HFC tensor is relatively insensitive to spin polarization. Differences between the GGA and the hybrid functionals are thus small (Table 1). Explicitly computed SO corrections to the anisotropic part are small but reduce the deviation from experiment in all cases. The semiemprical SO corrections from ref 2 appear too large relative to the present results in all four cases.

As found previously,[2,3] the NR contribution (FC term) to the isotropic HFC is much more sensitive to the functional, as it depends crucially on the description of spin polarization. The B3PW91 hybrid functional provides more core−shell spin polarization and thus produces more negative spin density at the metal nucleus than the BP86 GGA (^{61}Ni has a negative nuclear *g* value, and the overall HFC exhibits thus a reversed sign). The SO corrections are also larger at B3PW91 level, consistent with the B3LYP vs BP86 comparison of Neese.[10] Overall, the B3PW91 results appear to agree well with experiment when including the explicit B3PW91 SO corrections. For the isotropic HFCs, the semiempirical SO corrections applied in ref 2 appear in all cases exaggerated and produce overall worse agreement with experiment compared to the corrections computed here explicitly. As discussed previously,[2,3] this may partly be due to the neglect of hybridization between metal d, s, and p orbitals, the use of Mulliken analyses in estimating d populations, and other approximations used in applying the classical perturbation formulas. In particular, we had argued that the SO correction for $[Mn(CO)_5]$ is probably overestimated due to the small coefficient of the d_{z^2} orbital in the SOMO.[2,3] This is confirmed by the present, much smaller SO corrections. Similarly, the SO corrections were thought to be too large for $[Ni(CO)_3H]$, as confirmed by the present results. Significantly smaller SO corrections in the present, more quantitative treatment are also obvious for $[Co(CO)_4]$.

4.2. Copper Complexes. Neese has studied a number of different copper complexes with O, N, and S ligands to validate his approach for calculating HFC tensors with semiempirical SO operators, using the BP86 and B3LYP functionals.[10] Here we used our own approach with the BP86 GGA functional and the B3PW91 hybrid functional for the same set of species (see Table 2).

In these complexes, SO corrections are obviously of the same order of magnitude as the NR contributions. Their inclusion is thus absolutely mandatory for accurate calculations of the metal HFC tensors. Scalar relativistic effects, which are not incorporated here, are expected to give additionally contributions in the range of 5−10%.[40]

With SO corrections taken into account, results with hybrid functionals are a significant improvement over the GGA results when compared to experiment, both in the present study and in Neese's investigation (the sign of the experimental **A** tensor was not determined in all cases but is always negative where known). This is due to enhanced core−shell spin-polarization contributions to the FC term (cf. ref 2), but also to enhanced SO contributions. The general improvement of the agreement with experiment by inclusion of SO corrections is shown clearly for both isotropic and dipolar components of the HFC tensors in Figures 1 and 2, albeit this improvement is far less obvious when using the BP86 GGA functional (Figure 1) than with the

TABLE 2: Metal Hyperfine Coupling Tensors for Various Copper Complexes[a]

		isotropic part				dipolar (anisotropic) part			
complex[b]		A^{FC}	A^{PC}	total	exp[c]	A^{dip}	$A^{dip,2}$	total	exp[c]
$[Cu(acac)_2]$	ref 10								
	BP86	−271	88	−163		−400, 198, 203	83, −38, −44	−317, 160, 159	
	B3LYP	−339	129	−210		−487, 241, 246	118, −57, −61	−369, 184, 185	
	this work:				−223[46]				−327, 163, 163
	BP86	−265	70	−195		−346, 172, 175	67, −32, −35	−280, 139, 141	
	B3PW91	−366	110	−256		−461, 225, 237	101, −49, −53	−360, 175, 185	
$[Cu(NH_3)_4]^{2+}$	ref 10								
	BP86	−280	82	−198		−419, 210, 210	75, −37, −37	−344, 173, 173	
	B3LYP	−340	113	−227		−478, 239, 239	102, −51, −51	−357, 178, 178	
	this work:				−243[47]				−343, 172, 172
	BP86	−268	87	−181		−387, 193, 193	77, −38, −39	−310, 155, 155	
	B3PW91	−348	126	−222		−468, 229, 239	111 , −54, −57	−357, 174, 182	
$[Cu(dtc)_2]$	ref 10								
	BP86	−198	41	−157		−278, 138, 141	37, −18, −17	−241, 120, 124	
	B3LYP	−257	56	−201		−322, 153, 163	50, −26, −25	−272, 127, 138	
	this work:				−236[48]				−240, 111, 129
	BP86	−218	51	−167		−257, 127, 130	46, −24, −22	−211, 104, 108	
	B3PW91	−309	72	−237		−311, 154, 157	66, −34, −32	−245, 120, 125	
$[Cu(KTS)]$	ref 10								
	BP86	−223	56	−167		−325, 162, 163	47, −26, −22	−278, 136, 141	
	B3LYP	−292	81	−211		−387, 192, 195	70, −37, −33	−317, 155, 162	
	this work:				−263[49]				−306, 153, 153
	BP86	−239	68	−171		−327, 162, 165	58, −30, −28	−269, 132, 137	
	B3PW91	−331	100	−231		−403, 198, 205	86, −44, −42	−317, 154, 163	
$[Cu(en)_2]2+$	ref 10								
	BP86	−280	78	−202		−395, 197, 198	72, −36, −36	−323, 161, 162	
	B3LYP	−347	109	−238		−458, 228, 229	100, −49, −50	−358, 179, 179	
	this work:				−258[47]				−350, 175, 175
	BP86	−288	79	−209		−386, 193, 192	71, −36, −35	−314, 157, 157	
	B3PW91	−379	112	−267		−455, 226, 229	102, −50, −52	−354, 176, 178	
$[Cu(gly)_2]$	ref 10								
	BP86	−229	79	−150		−391, 176, 215	74, −31, −43	−317, 145, 172	
	B3LYP	−315	116	−199		−472, 203, 270	105, −42, −64	−367, 161, 206	
	this work:				−205[47]				−324, 162, 162
	BP86	−243	74	−169		−361, 159, 202	67, −28, −39	−294, 131, 163	
	B3PW91	−344	113	−231		−460, 189, 271	101, −38, −64	−359, 151, 208	
$[Cu(iz)_4]2+$	ref 10								
	BP86	−233	93	−140		−404, 199, 205	84, −42, −41	−320, 157, 164	
	B3LYP	−291	133	−158		−483, 238, 245	118, −59, −59	−365, 179, 186	
	this work:				−179[47]				−357, 179, 179
	BP86	−237	93	−143		−389, 194, 195	83, −42, −41	−306, 152, 154	
	B3PW91	−312	137	−175		−476, 237, 239	120, −61, −59	−356, 177, 179	
$[Cu(mnt)_2]^{2-}$	ref 10								
	BP86	−191	37	−154		−267, 132, 136	31, −17, −15	−236, 115, 121	
	B3LYP	−252	53	−199		−323, 163, 160	47, −22, −24	−276, 141, 136	
	this work:				−238[50]				−244, 121, 124
	BP86	−203	40	−163		−257, 126, 130	35, −18, −17	−222, 108, 114	
	B3PW91	−291	57	−234		−311, 154, 157	51, −26, −25	−260, 128, 133	
$[Cu(sac)_2]$	ref 10								
	BP86	−215	79	−136		−402, 187, 215	68, −27, −42	−334, 160, 173	
	B3LYP	−275	112	−163		−486, 240, 246	98, −43, −54	−388, 197, 192	
	this work:				−227[51]				−328, 164, 164
	BP86	−250	84	−166		−394, 199, 195	75, −42, −33	−319, 157, 162	
	B3PW91	−337	124	−213		−478, 240, 238	107, −58, −50	−371, 183, 188	

[a] MAG-ReSpect calculations, (15s11p6d)/[9s7p4d] basis set for Cu, BII basis sets for the main group elements. [b] For Cartesian coordinates of the complexes, see Supporting Information (Table 5S). [c] The sign of the experimental **A** tensor was not determined in all cases but is always negative where known. Therefore the signs of the experimental **A** tensors were adapted to the calculated ones.

B3PW91 hybrid functional (Figure 2). No problems with spin contamination are encountered, and thus the use of hybrid functionals appears to be justified.

Though our BP86 results agree closely with those of Neese, our B3PW91 data deviate notably from his B3LYP results, particularly for the isotropic component. In general our B3PW91 data for these tensor components appear to be in better agreement with experiment, whereas the dipolar components are similar (see Table 2). Closer inspection reveals that the differences arise mainly from the FC term and not so much from the SO corrections. Though we have used slightly different basis sets than Neese, a number of test calculations with his preferred basis set combinations indicated only minor differences. Additional B3LYP calculations (see Supporting Information Table 5S) showed that our better agreement with experiment reflects an overall somewhat better performance of the B3PW91 functional for the FC term compared to B3LYP. Similar, moderate effects of correlation functionals in transition metal HFC calculations have been noted in previous work.[2]

Figure 3 plots Neese's SO corrections (PC and "dip,2" contribution) against ours at the B3PW91 level. The overall good agreement confirms an adequate choice of the semiempirical

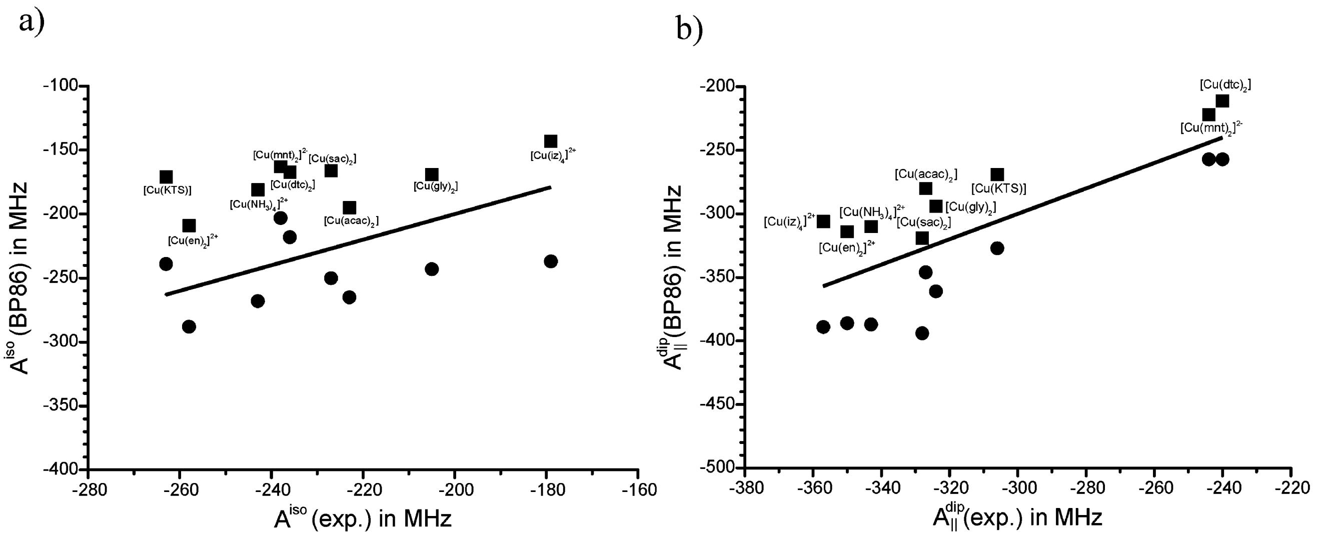

Figure 1. BP86 results for metal hyperfine tensors (MHz) of copper complexes: (a) Isotropic contribution A^{iso}; (b) dipolar contribution A^{dip} (parallel component). Circles are NR results; squares include SO corrections. Straight lines indicate ideal agreement with experiment.

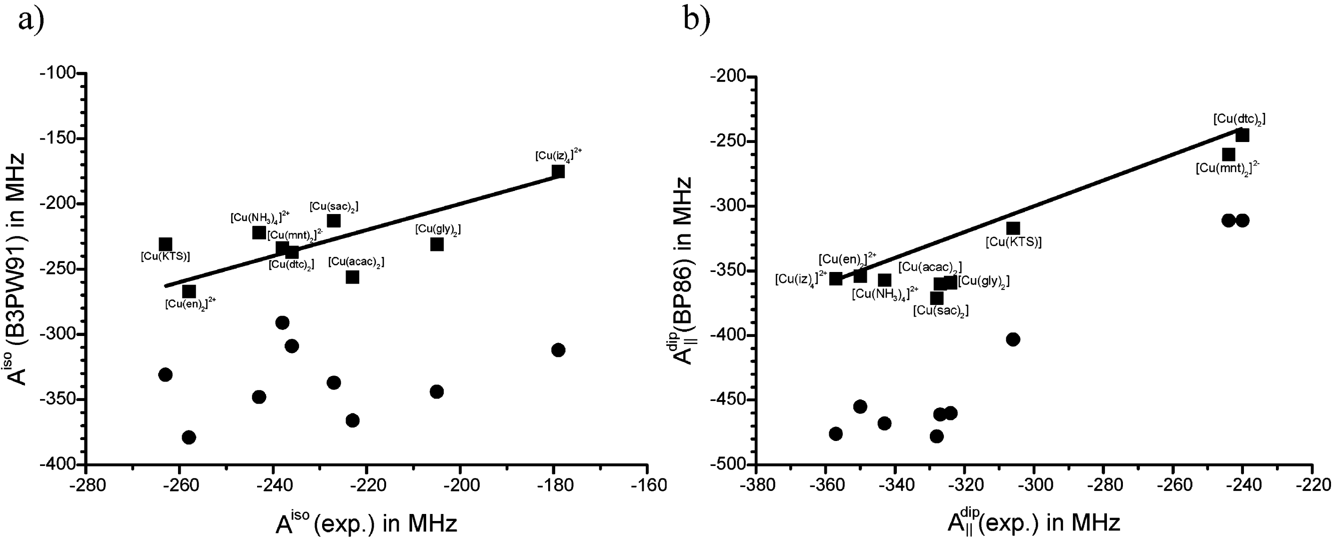

Figure 2. B3PW91 results for metal hyperfine tensors (MHz) of copper complexes: (a) Isotropic contribution A^{iso}; (b) dipolar contribution A^{dip} (parallel component). Circles are NR results; squares include SO corrections. Straight lines indicate ideal agreement with experiment.

SO parameters by Neese for the 3d metal copper. The advantage of our approach lies in the fact that no parametrization is needed. Thus, the present method is more flexible regarding its use throughout the periodic table, and it should perform also more uniformly when the bonding situation covers a wide range (and thus the SO coupling may become quite different from the atomic state chosen for a particular semiempirical parametrization).

4.3. Manganese Complexes. In view of the importance of manganese complexes in bioinorganic chemistry and in molecular magnetism, three manganese complexes were also included in the study: The low-spin $[Mn(CN)_5NO_2]^{2-}$ and $[Mn(CO)_5]$ ($S = {}^1/_2$) and the high-spin $[Mn(H_2O)_6]^{2+}$ ($S = {}^5/_2$). Compared to the copper complexes SO corrections play smaller role in this case (see Table 3). They are by 1 or 2 orders of magnitudes smaller than the FC and dipolar contributions. For $[Mn(CN)_5NO_2]^{2-}$, calculations with the B3PW91 hybrid functional suffer from large spin contamination ($S^2 = 1.465$), and the results have thus to be viewed with care. In the other two complexes, no problems occur with spin contamination, and the B3PW91 hybrid functional improves agreement with experiment over the BP86 results (see also ref 2).

4.4. Use of SO-ECPs on Heavy Atoms. As in ref 12, we have also considered the use of SO-ECPs as a means to incorporate both SR and SO effects for the HFC tensors of light nuclei in the neighborhood of heavy atoms. Due to the nodeless character of the pseudovalence orbitals obtained, this procedure is not straightforwardly applicable to the calculation of HFC tensors of the heavy atom itself. Table 4 shows a comparison of SO-ECP and all-electron results for the light nuclei (indcated by the italic letters) in six diatomics (Ga*O*, In*O*, Rh*C*, *N*Br, *N*I, I*O*$_2$). The BP86 results are compared to the deMon calculations of ref 12, in which Coulomb and exchange-correlation potential were fitted by auxiliary basis sets, in contrast to the present work. In addition, we provide also results of B3PW91 calculations.

First of all, we note that the agreement between all-electron and ECP calculations is as found in ref 12, thus validating the

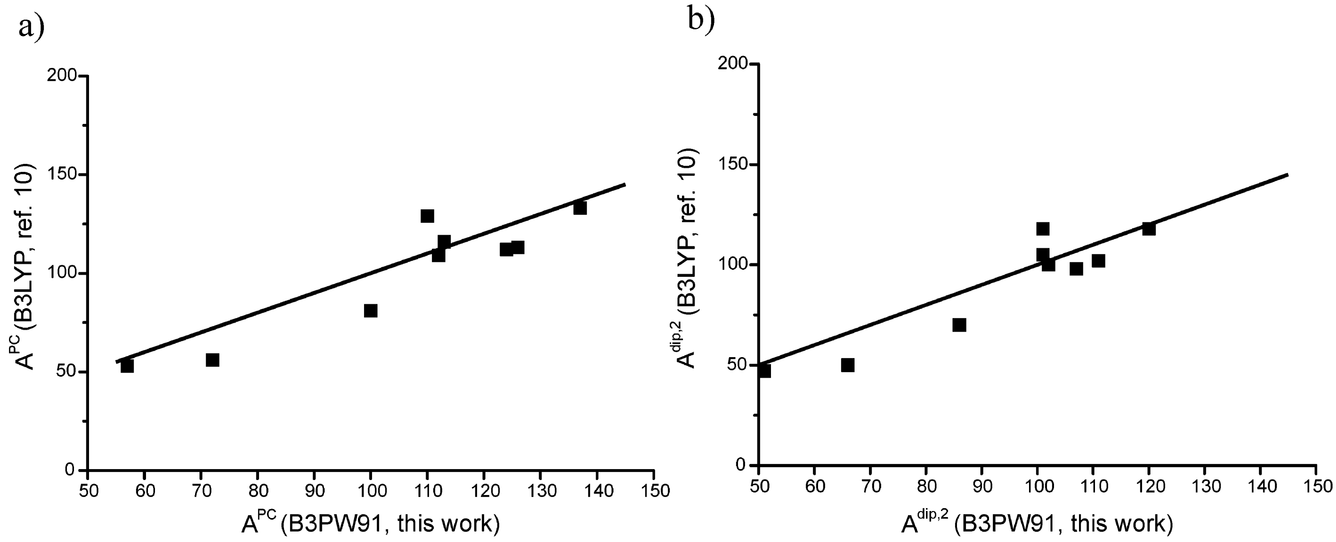

Figure 3. Comparison between present work (AMFI approximation) and Neese's results (semiempirical SO operators; see ref 10) for SO corrections to metal HFC tensors (MHz) in copper complexes: (a) pseudocontact (PC) contribution; (b) anisotropic (dip, 2) contribution.

TABLE 3: Metal Hyperfine Coupling Tensors (MHz) for Manganese Complexes[a]

		isotropic part				dipolar (anisotropic) part			
complex		A^{FC}	A^{PC}	total	exp	A^{dip}	$A^{dip,2}$	total	exp
$[Mn(CN)_5NO_2]^{2-}$	BP86	−148	−15	−164	−218[52]	−81	−2	−83	−115[52]
	B3PW91	−258	−21	−279		−56	−3	−59	
$[Mn(CO)_5]$	BP86	6	2	8	−2.8, 0.6, 5.6[45]	96	−2	94	90(8)−92(6)[45]
	B3PW91	−4	2	−2		95	−2	93	
$[Mn(H_2O)_6]^{2+}$	BP86	−163	−3	−166	−245[53]	0	0	0	0[53]
	B3PW91	−196	−3	−199		1	0	1	

[a] MAG-ReSpect calculations, (15s11p6d)/[9s7p4d] basis set for Mn, BII basis sets for the main group elements.

SO-ECP implementation in our new code. The only appreciable discrepancies between all-electron and ECP results are seen for the FC contributions in InO and RhC. These differences have been rationalized by SR effects, which are included in the ECP calculations but not in the all-electron results.[12] Overall, SO-ECPs are an efficient alternative to an all-electron treatment when heavy atoms are involved in a molecule and the **A** tensor of a light atom is needed.

Agreement between the present BP86 results and those of ref 12 is generally good for the NR contributions, even though there are minor discrepancies in the FC term. This suggests that the approximations of the deMon implementation (see introduction) did not affect the NR results dramatically. In contrast, the SO contributions are notably larger for GaO and RhC, and particularly for InO, in the present results. These differences are due to the fact that in ref 12 Malkin's sum-over-states density functional perturbation theory correction terms[23] were used, whereas in the present work those correction terms were not applied.

In going from the BP86 to the B3PW91 functional, the dipolar and SO contributions increase moderately, whereas the FC term is enhanced more notably, as found for transition metal systems. However, in contrast to the latter, the overall comparison with experiment is not generally improved by switching to the B3PW91 hybrid functional. Indeed, the BP86 results appear to be closer to experiment for GaO, InO, and RhC (SO-ECP results in the latter two cases), whereas the B3PW91 results appear overall superior for NBr and NI. We should note that experimental data have been recorded either in matrix (GaO, InO, RhC), in the gas-phase (NI, NBr), or embedded in a crystal (IO_2).

5. Conclusions

Spin−orbit (SO) corrections to metal hyperfine coupling tensors may be significant already for 3d metal complexes, as amply confirmed by results for the series of copper complexes investigated. In these cases, the addition of SO corrections brings computed and experimental HFC tensors into excellent agreement (at the B3PW91 hybrid DFT level). DFT combined with second-order perturbation theory provides an efficient and adequate tool to include SO effects into HFC tensor calculations, provided the SO corrections are not too large for a perturbation theoretical treatment. In particular, a treatment with an unrestricted Kohn−Sham state and perturbational inclusion of spin−orbit coupling is well-suited to include spin polarization straightforwardly.

The great advantage of the present implementation over alternative ones[2,9,10] is the use of accurate and efficient nonempirical approximations to the microscopic SO Hamiltonian. This allows a flexible and reliable treatment throughout the Periodic Table and for very different bonding situations, whereas semiempirical SO operators may be accurate in some cases but difficult to parametrize in others. SO-ECPs on heavy atoms offer a convenient way of including also heavy-atom scalar relativistic effects in valence-only calculations when dealing with the HFC tensors of light nuclei in the neighborhood of these heavy atoms. Inclusion of scalar relativistic *and* SO effects for the HFCs of the heavy nuclei themselves requires a suitable relativistic all-electron approach. We are currently testing approaches based on the Douglas−Kroll−Hess Hamiltonian to achieve this task.[41] The perturbation theoretical treatment of SO effects based on a

TABLE 4: Hyperfine Coupling Tensors (MHz) for Light Nuclei in Selected Diatomics[a]

molecule		$\mathbf{A}^{NR}$		$\mathbf{A}^{SO}$		total **A** tensor	
		FC	dip	PC	dip, 2	iso	dip
Ga*O*	BP86, SOECP, deMon[b]	9.11	−81.25	5.84	−2.85	14.95	−84.09
	BP86, AMFI, deMon[b]	9.89	−78.66	6.07	−3.00	15.96	−81.66
	BP86, SOECP[16]	8.66	−81.35	7.91	−4.22	16.57	−85.57
	BP86, AMFI	9.57	−78.58	8.26	−4.07	17.83	−82.65
	B3PW91, SOECP[16]	14.40	−86.71	8.20	−4.63	22.61	−90.57
	B3PW91, AMFI	15.92	−84.01	8.55	−4.10	24.47	−88.11
	exp[54]					8.33	−76.7
In*O*	BP86, SOECP, deMon[b]	4.97	−85.09	19.59	−9.35	24.56	−94.44
	BP86, AMFI, deMon[b]	7.63	−78.25	19.01	−9.18	26.64	−87.43
	BP86, SOECP[16]	5.24	−85.32	27.65	−13.53	32.88	−98.45
	BP86, AMFI	7.27	−77.83	26.37	−12.89	33.63	−90.72
	B3PW91, SOECP[16]	8.41	−92.04	31.49	−15.20	39.90	−106.75
	B3PW91, AMFI	11.12	−85.53	30.03	−14.31	41.14	−99.84
	exp[54]					34.7	−131.3
Rh*C*	BP86, SOECP, deMon[b]	63.79	17.66	3.06	−1.62	66.85	16.04
	BP86, AMFI, deMon[b]	37.67	19.71	4.63	−2.39	42.30	17.32
	BP86, SOECP[13]	64.18	16.65	3.51	−1.86	67.69	14.79
	BP86, AMFI	37.75	19.22	5.97	−3.07	43.72	16.15
	B3PW91, SOECP[13]	46.81	19.44	4.81	−2.54	51.62	16.90
	B3PW91, AMFI	23.97	22.21	8.69	−4.44	32.67	17.77
	exp[55]					66.3	11.3
*N*Br	BP86, SOECP, deMon[b]	5.51	−20.25	1.21	−1.52	6.72	−21.77
	BP86, AMFI, deMon[b]	5.47	−20.25	1.26	−1.58	6.73	−21.83
	BP86, SOECP[14]	6.24	−20.77	1.41	−1.63	7.65	−22.40
	BP86, AMFI	5.94	−20.24	1.42	−1.74	7.36	−21.98
	B3PW91, SOECP[14]	11.14	−21.35	1.49	−1.51	12.63	−22.86
	B3PW91, AMFI	10.76	−20.91	1.50	−1.61	12.26	−22.52
	exp[56]					21.39	−20.63
*N*I	BP86, SOECP, deMon[b]	2.98	−19.45	3.14	−3.61	6.12	−23.06
	BP86, AMFI, deMon[b]	2.98	−19.40	3.06	−3.62	6.04	−23.02
	BP86, SOECP[14]	2.94	−19.53	3.42	−3.98	6.36	−23.51
	BP86, AMFI	3.52	−19.38	3.46	−4.07	6.96	−23.45
	B3PW91, SOECP[14]	6.49	−20.01	3.69	−3.59	10.18	−23.60
	B3PW91, AMFI	7.16	−19.96	3.71	−3.65	10.87	−23.61
	exp[57]					20.44	−21.31
IO_2	BP86, SOECP, deMon[b,c]		−108.4		8.05		−100.3
		−4.79	54.44	−7.73	−28.85	−12.52	25.10
			53.95		20.80		75.23
	BP86, AMFI, deMon[b,c]		−106.3		8.19		−98.13
		−4.96	53.71	−7.92	−28.85	−12.88	23.78
			52.62		20.66		74.35
	BP86, SOECP[14]		−108.9		0.29		−113.29
		−4.65	54.55	−8.31	−38.10	−12.96	11.80
			54.37		12.87		62.59
	BP86, AMFI		−105.83		8.74		−97.10
		−5.47	52.71	−8.47	−30.99	−13.94	21.72
			53.12		22.25		75.37
	B3PW91, SOECP[14]		−112.74		13.04		−99.70
		−13.35	56.70	−12.62	−32.57	−25.97	24.12
			56.04		19.53		75.57
	B3PW91, AMFI		−110.26		12.94		−97.32
		−14.16	55.13	−12.55	−33.61	−26.71	21.52
			55.13		20.68		75.80
	exp[58]						−64.5
						−37.4	15.7
							48.8

[a] Gaussian98 calculations for SCF part (ultrafine grid, option of the Gaussian98 program) and MAG calculations for HFC tensors, BIII basis sets for the italic elements, FIII basis sets or Stuttgart pseudopotentials (in case of SOECP-calculations) as indicated for the other elements. [b] Previous deMon calculations[12] with fitting of electron density and exchange-correlation potential. [c] Small discrepancies in the sum of A^{dip} (NR-part) and $A^{dip,2}$ to A^{dip}(total) are due to antisymmetric contributions to $\mathbf{A}^{SO}$ (cf. ref 12).

one-component wave function remains a valid option also in this case (provided again that the SO effects are not too large).

In the case of transition metal complexes, we confirm Neese's observation that hybrid functionals tend to enhance the SO contributions and lead to improved agreement with experiment compared to GGA functionals. We emphasize, however, that care has to be taken in cases where exact-exchange admixture leads to appreciable spin contamination.[2] Our present results for main-group diatomics allow no general statement to be made with respect to superior performance of one or the other type of functionals.

Acknowledgment. This study has been supported by the graduate college "Moderne Methoden der magnetischen Resonanz in der Materialforschung" at Universität Stuttgart, Deutsche Forschungsgemeinschaft (Priority Program SP1051, "High-Field EPR", project Ka1187/4), and by Fonds der Chemischen Industrie. C.R. thanks also Studienstiftung des Deutschen Volkes for a scholarship. J.V. is an Academy Fellow of the Academy of Finland and has additionally been supported by the Emil Aaltonen Foundation. O. L Malkina and V. G. Malkin (Bratislava) are gratefully acknowledged for their invaluable contributions to the development of the MAG-ReSpect code. We are also thankful to F. Neese (Mülheim) for sharing with us his optimized structures of the copper complexes for comparison.

Supporting Information Available: Tables of optimized structures (Cartesian coordinates) of studied copper complexes and additional first-order HFC calculations with B3LYP. This material is available free of charge via the Internet at http://pubs.acs.org.

References and Notes

(1) Kaupp, M.; Bühl, M.; Malkin, V. G. *Calculation of NMR and EPR Parameters: Theory and Applications*; Wiley-VCH: Weinheim, 2004.

(2) Munzarová, M.; Kaupp, M. *J. Phys. Chem. A* **1999**, *103*, 9966.

(3) Munzarová, M. L.; Kubáček, P.; Kaupp, M. *J. Am. Chem. Soc.* **2000**, *122*, 11900.

(4) Quiney, H. M.; Belanzoni, P. *Chem. Phys. Lett.* **2002**, *353*, 253.

(5) Lenthe, E. v.; Avoird, A. v. d.; Wormer, P. E. S. *J. Chem. Phys.* **1998**, *108*, 4783.

(6) a) Douglas, M.; Kroll, N. M. *Ann. Phys. (N. Y.)* **1974**, *82*, 89. (b) Hess, B. A. *Phys. Rev. A* **1985**, *32*, 3742. (c) Hess, B. A. *Phys. Rev. A* **1986**, *32*, 3742.

(7) Stein, M.; Lenthe, E. v.; Baerends, E. J.; Lubitz, W. *J. Phys. Chem. A* **2001**, *105*, 416.

(8) Belanzoni, P.; Lenthe, E. v.; Baerends, E. J. *J. Chem. Phys.* **2001**, *114*, 4421.

(9) Belanzoni, P.; Baerends, E. J.; Asselt, S. v.; Langewen, P. B. *J. Phys. Chem.* **1995**, *99*, 13094.

(10) Neese, F. *J. Chem. Phys.* **2003**, *118*, 3939.

(11) Geurts, P. J. M.; Bouten, P. C. P.; van der Avoird, A. *J. Chem. Phys.* **1980**, *73*, 1306. See also: Neese, F. *J. Phys. Chem. A* **2001**, *105*, 4290.

(12) Arbuznikov, A. V.; Vaara, J.; Kaupp, M. *J. Chem. Phys.* **2004**, *120*, 2127.

(13) Hess, B. A.; Marian, C. M.; Wahlgren, U.; Gropen, O. *Chem. Phys. Lett.* **1996**, *251*, 365.

(14) Andrae, D.; Häussermann, U.; Dolg, M.; Stoll, H.; Preuss, H. *Theor. Chim. Acta* **1990**, *77*, 123.

(15) Bergner, A.; Dolg, M.; Küchle, W.; Stoll, H.; Preuss, H. *Mol. Phys.* **1993**, *80*, 1431.

(16) Metz, B.; Stoll, H.; Dolg, M. *J. Chem. Phys.* **2000**, *113*, 2563.

(17) See: http://www.theochem.uni-stuttgart.de/pseudopotentiale.

(18) (a) Salahub, D. R.; Fournier, R.; Mlynarski, P.; Papai, I.; St-Amant, A.; Ushio, J. In *Density Functional Methods in Chemistry*; Labanowski, J., Andzelm, J., Eds.; Springer: New York, 1991. (b) St-Amant, A.; Salahub, D. R. *Chem. Phys. Lett.* **1990**, *169*, 387.

(19) Malkin, V. G.; Malkina, O. L.; Eriksson, L. A.; Salahub, D. R. In *Modern Density Functional Theory: A Tool for Chemistry*; Politzer, P., Seminario, J. M., Eds.; Theoretical and Computational Chemistry Vol. 2; Elsevier: Amsterdam, 1995; p 273.

(20) Malkin, V. G.; Malkina, O. L.; Reviakine, R.; Arbuznikov, A. V.; Kaupp, M.; Schimmelpfennig, B.; Malkin, I.; Helgaker, T.; Ruud, K. MAG-ReSpect (Version 1.1), 2003.

(21) Harriman, J. E. *Theoretical Foundations of Electron Spin Resonance*; Academic Press: New York, 1978.

(22) Kaupp, M.; Reviakine, R.; Malkina, O. L.; Arbuznikov, A.; Schimmelpfennig, B.; Malkin, V. G. *J. Comput. Chem.* **2002**, *23*, 794.

(23) Malkin, V. G.; Malkina, O. L.; Casida, M. E.; Salahub, D. R. *J. Am. Chem. Soc.* **1994**, *116*, 5898.

(24) Perdew, J. P.; Wang, Y. *Phys. Rev. B* **1986**, *33*, 8800.

(25) Perdew, J. P.; Wang, Y. *Phys. Rev. B* **1986**, *33*, 8822; **1986**, *34*, 7406.

(26) Becke, A. D. *Phys. Rev. A* **1988**, *38*, 3098.

(27) Becke, A. D. *J. Chem. Phys.* **1993**, *98*, 5648.

(28) Perdew, J. P. In *Electronic Structure of Solids '91*; Ziesche, P., Eschring, H., Eds.; Akademie Verlag: Berlin, 1991.

(29) Stephens, P. J.; Devlin, F. J.; Chabalowski, C. F.; Frisch, M. J. *J. Phys. Chem.* **1994**, *98*, 11623.

(30) Frisch, M. J.; Trucks, G. W.; Schlegel, H. B.; Scuseria, G. E.; Robb, M. A.; Cheeseman, J. R.; Zakrzewski, V. G.; Montgomery, J. A., Jr.; Stratmann, R. E.; Burant, J. C.; Dapprich, S.; Millam, J. M.; Daniels, A. D.; Kudin, K. N.; Strain, M. C.; Farkas, O.; Tomasi, J.; Barone, V.; Cossi, M.; Cammi, R.; Mennucci, B.; Pomelli, C.; Adamo, C.; Clifford, S.; Ochterski, J.; Petersson, G. A.; Ayala, P. Y.; Cui, Q.; Morokuma, K.; Malick, D. K.; Rabuck, A. D.; Raghavachari, K.; Foresman, J. B.; Cioslowski, J.; Ortiz, J. V.; Baboul, A. G.; Stefanov, B. B.; Liu, G.; Liashenko, A.; Piskorz, P.; Komaromi, I.; Gomperts, R.; Martin, R. L.; Fox, D. J.; Keith, T.; Al-Laham, M. A.; Peng, C. Y.; Nanayakkara, A.; Gonzalez, C.; Challacombe, M.; Gill, P. M. W.; Johnson, B.; Chen, W.; Wong, M. W.; Andres, J. L.; Gonzalez, C.; Head-Gordon, M.; Replogle, E. S.; Pople, J. A. *Gaussian 98*, revision A.7; Gaussian, Inc.: Pittsburgh, PA, 1998.

(31) Kutzelnigg, W.; Fleischer, U.; Schindler, M. In *NMR Basic Principles and Progress*; Diehl, P., Fluck, E., Günther, H., Kosfeld, R., Seelig, J., Eds.; Springer-Verlag: Berlin, 1990; Vol. 23.

(32) Huzinaga, S. *Approximate Atomic Functions*; University of Alberta: Alberta, ON, Canada, 1971.

(33) Fægri, K., Jr., personal communication. See also http://folk.uio.no/knutf/bases/one.

(34) Schimmelpfennig, B. AMFI, Atomic Spin−Orbit Mean-Field Integral Program, Stockholms Universitet, Sweden, 1996.

(35) Malkina, O. L.; Schimmelpfennig, B.; Kaupp, M.; Hess, B. A.; Chandra, P.; Wahlgren, U.; Malkin, V. G. *Chem. Phys. Lett.* **1998**, *296*, 93.

(36) Malkina, O. L.; Vaara, J.; Schimmelpfennig, B.; Munzarová, M.; Malkin, V. G.; Kaupp, M. *J. Am. Chem. Soc.* **2000**, *122*, 9206.

(37) Ahlrichs, R.; Bär, M.; Häser, M.; Horn, H.; Kölmel, C. *Chem. Phys. Lett.* **1989**, *162*, 165. See also: Ahlrichs, R.; von Arnim, M. In *Methods and Techniques in Computational Chemistry: METECC-95*; Clementi, E., Corongiu, G., Eds.; Club Européen MOTECC: Cagliari, 1995; p 509.

(38) Schäfer, A.; Huber, C.; Ahlrichs, R. *J. Chem. Phys.* **1994**, *100*, 5829.

(39) (a) Eichkorn, K.; Treutler, O.; Öhm, H.; Häser, M.; Ahlrichs, R. *Chem. Phys. Lett.* **1995**, *240*, 283. (b) Eichkorn, K.; Weigend, F.; Treutler, O.; Ahlrichs, R. *Theor. Chem. Acc.* **1997**, *97*, 199.

(40) Pyykkö, P.; Pajanne, E.; Inokuti, M. *Int. J. Quantum Chem.* **1973**, *7*, 785.

(41) Malkin, I.; Malkina, O. L.; Malkin, V. L.; Kaupp, M. Manuscript in preparation.

(42) Fairhust, S. A.; Morton, J. R.; Preston, K. F. *J. Magn. Reson.* **1983**, *55*, 453.

(43) Morton, J. R.; Preston, K. F. *J. Chem. Phys.* **1984**, *81*, 5775.

(44) Lionel, T.; Morton, J. R.; Preston, K. F. *J. Chem. Phys.* **1982**, *76*, 234.

(45) Symons, M. C. R. *Organometallics* **1982**, *1*, 834.

(46) Maki, A. H.; McGarvey, B. R. *J. Chem. Phys.* **1958**, *29*, 31.

(47) Scholl, H. J.; Hüttermann, J. *J. Phys. Chem. A* **1992**, *96*, 9684.

(48) Keijzers, C. P.; Snaathorst, D. *Chem. Phys. Lett.* **1968**, *90*, 2288.

(49) Blumberg, W. E.; Peisach, J. *J. Chem. Phys.* **1968**, *49*, 1793.

(50) Kirmse, R.; Stach, J.; Dietzsch, W.; Hoyer, E. *Inorg. Chim. Acta* **1978**, *26*, L53.

(51) Maki, A. H.; McGarvey, B. R. *J. Chem. Phys.* **1958**, *29*, 35.

(52) Manoharan, T.; Gray, H. B. *Inorg. Chem.* **1966**, *5*, 823.

(53) Upreti, G. C. *J. Magn. Reson.* **1974**, *13*, 336.

(54) Knight, L. B., Jr.; Kirk, T. J.; Herlong, J.; Kaup, J. G.; Davidson, E. R. *J. Chem. Phys.* **1997**, *107*, 7011.

(55) Weltner, W., Jr. *Magnetic Atoms and Molecules*; Dover: New York, 1983.

(56) Sakamaki, T.; Okabayashi, T.; Tanimoto, M. *J. Chem. Phys.* **1998**, *109*, 7169.

(57) Sakamaki, T.; Okabayashi, T.; Tanimoto, M. *J. Chem. Phys.* **1999**, *111*, 6345.

(58) Byberg, J. R. *J. Chem. Phys.* **1988**, *88*, 2129.